Electronic Supplementary Material (ESI) for Inorganic Chemistry Frontiers.

Supporting Information

Bromide anion-triggered visible responsive metallogels based on squaramide complexes

Di Wu, Ruyong Jiang, Liang Luo, Zhen He, and Jingsong You**

I. General remarks

High-resolution mass spectra (HRMS) were obtained by a Waters-Q-TOF-Premier (ESI^+). Melting points (M.p.) were determined with XRC-1 without correction.

TBAF: tetrabutylammonium fluoride; TBAC: tetrabutylammonium chloride; TBAB: tetrabutylammonium bromide; TBAI: tetrabutylammonium iodide.

II. Gelation tests, structure and spectra

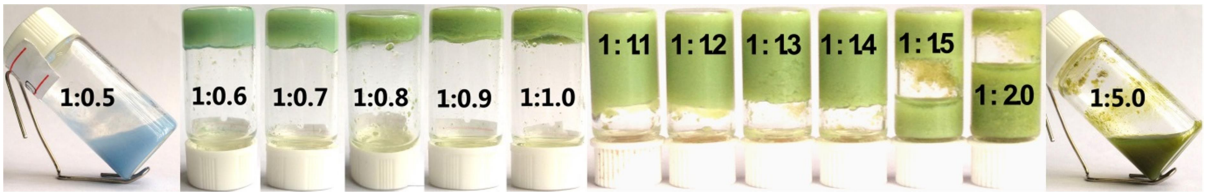

Figure S1. Optimization of gelator composition. Molar ratios of **L4**/$CuCl_2 \cdot 2H_2O$ are marked in the photos.

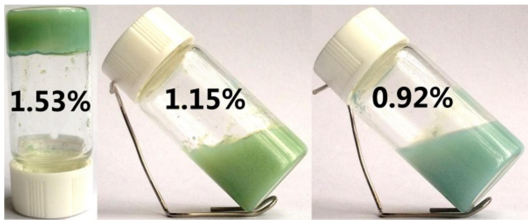

Figure S2. Optimization of the gelator concentration in MeOH. The weight concentration (wt%) of the gelator **L4**/$CuCl_2 \cdot 2H_2O$ (molar ratio = 1: 1) are marked in the photos.

Table S1 Gelation behavior of **L4**/$CuCl_2 \cdot 2H_2O$ (molar ratio = 1:1) in different solvents

Entry	Solvent (*v:v* if applicable)	Gelation behavior [a] (gelator concentration/wt% if applicable)
1	MeOH	G (1.53)
2	H_2O	P
3	DMF	P
4	DMSO	S
5	DMAc	P
6	MeOH/H_2O (1:0.1)	G (2.11)
7	MeOH/H_2O (1:0.2)	Gp
8	MeOH/H_2O (1:0.3)	P
9	MeOH/H_2O (1:0.4)	P

10	MeOH/EtOH (1:0.5)	G (1.50)
11	DMSO/MeOH (1:0.5)	G (1.27)
12	DMF/MeOH (1:0.5)	G (1.42)
13	DMAc/MeOH (1:0.5)	G (1.47)
14	DMSO/H_2O (1:0.5)	S
15	DMF/H_2O (1:0.5)	P
16	DMAc/H_2O (1:0.5)	P

[a] S: solution; G: steady gel; Gp: partial gel; P: precipitate.

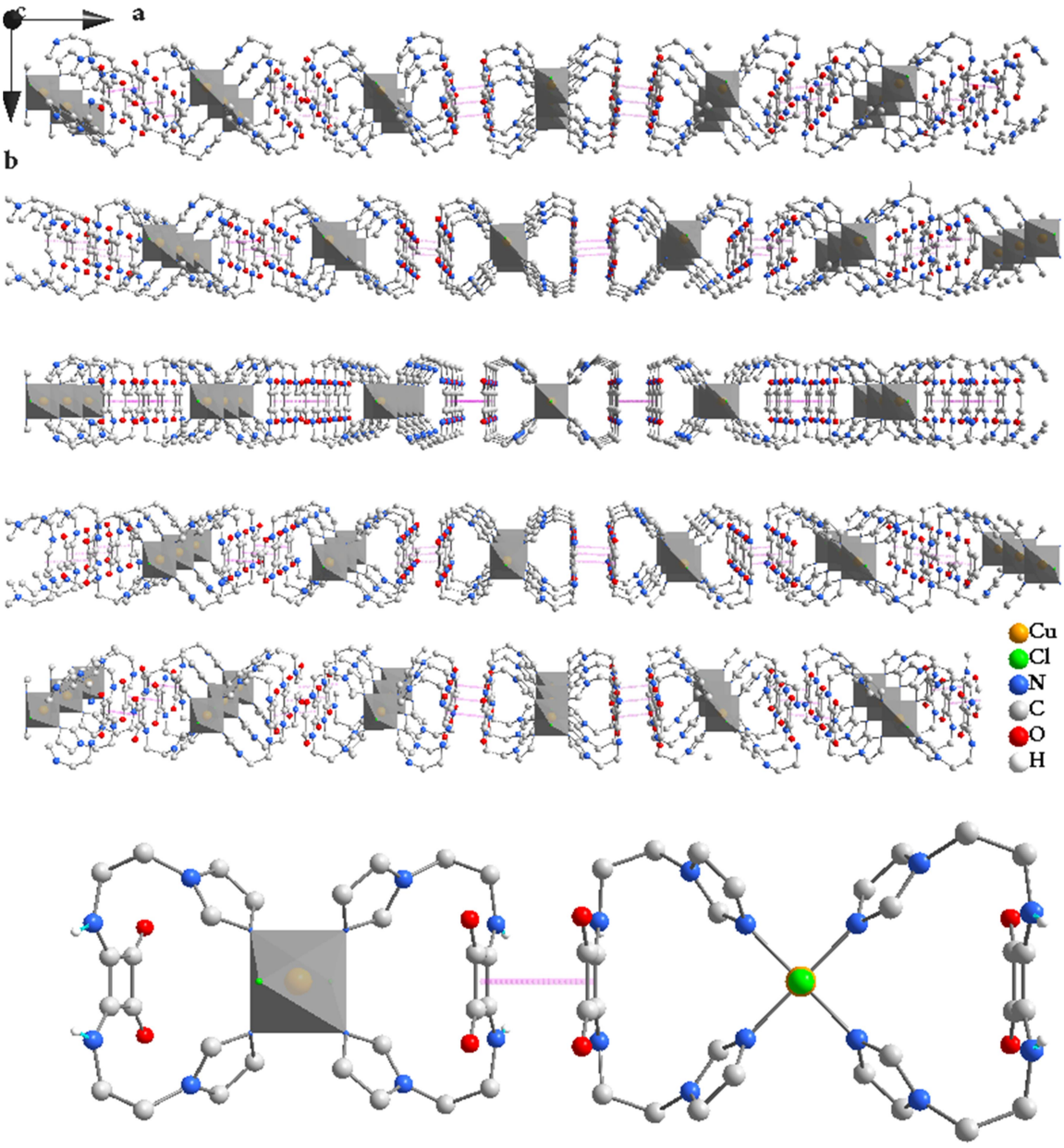

Figure S3 The packing structure of [Cu-**L4**$_2$]Cl_2 in crystals viewed along *c*-axis (top) with enlarged details (bottom).

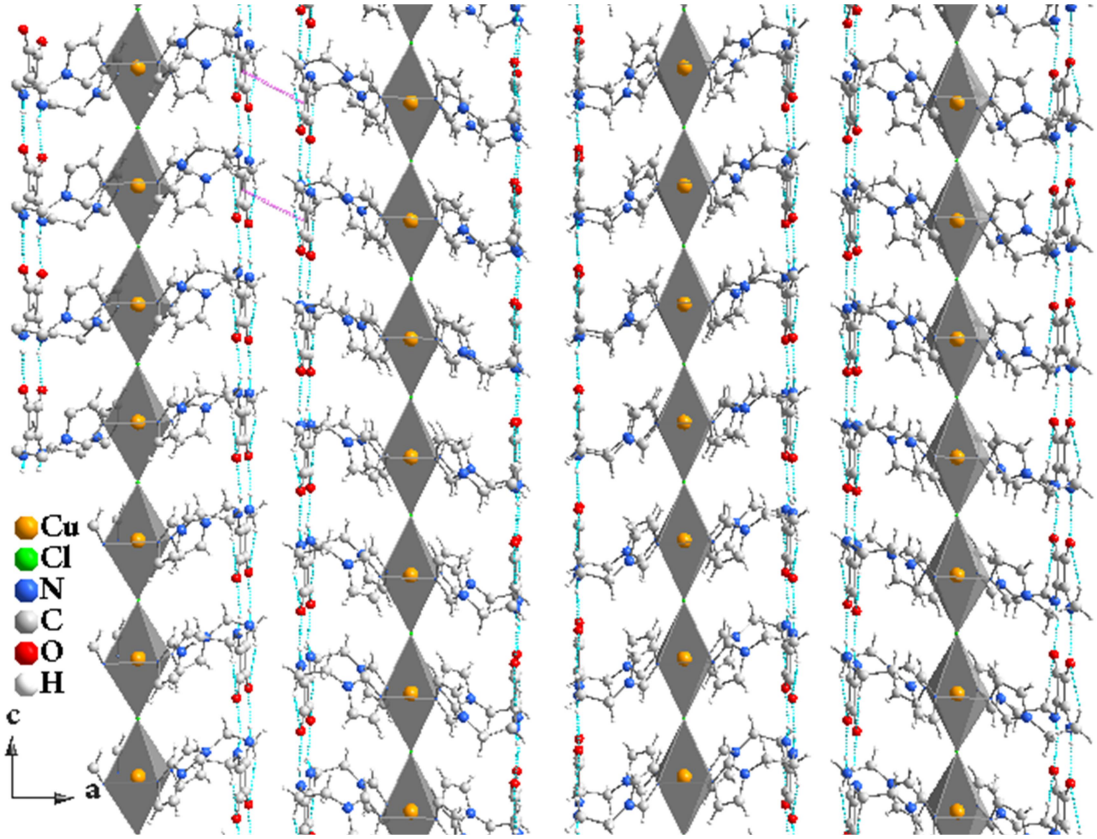

Figure S4 The packing structure of [Cu-**L4**$_2$]Cl_2 in crystals viewed along *b*-axis.

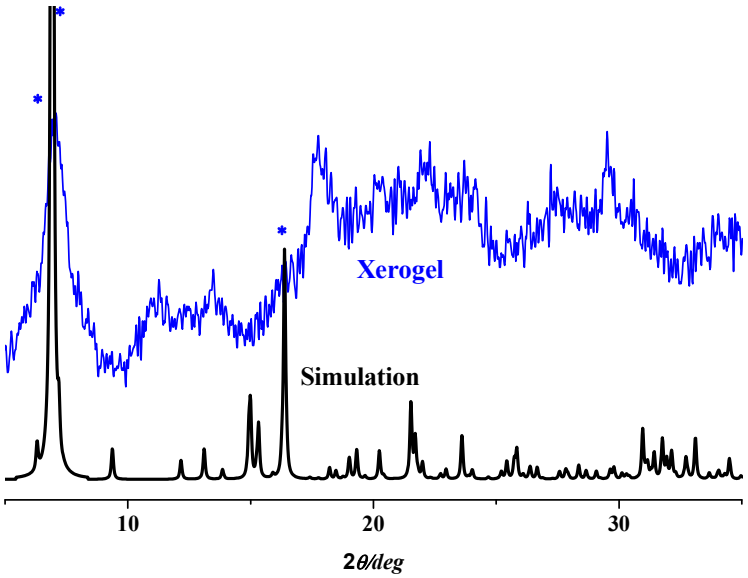

Figure S5 Measured PXRD patterns of **Gel-Br** xerogel (bottom) in comparison with the simulated single crystal XRD [Cu-**L4**$_2$]Br_2. Three peaks are marked with stars.

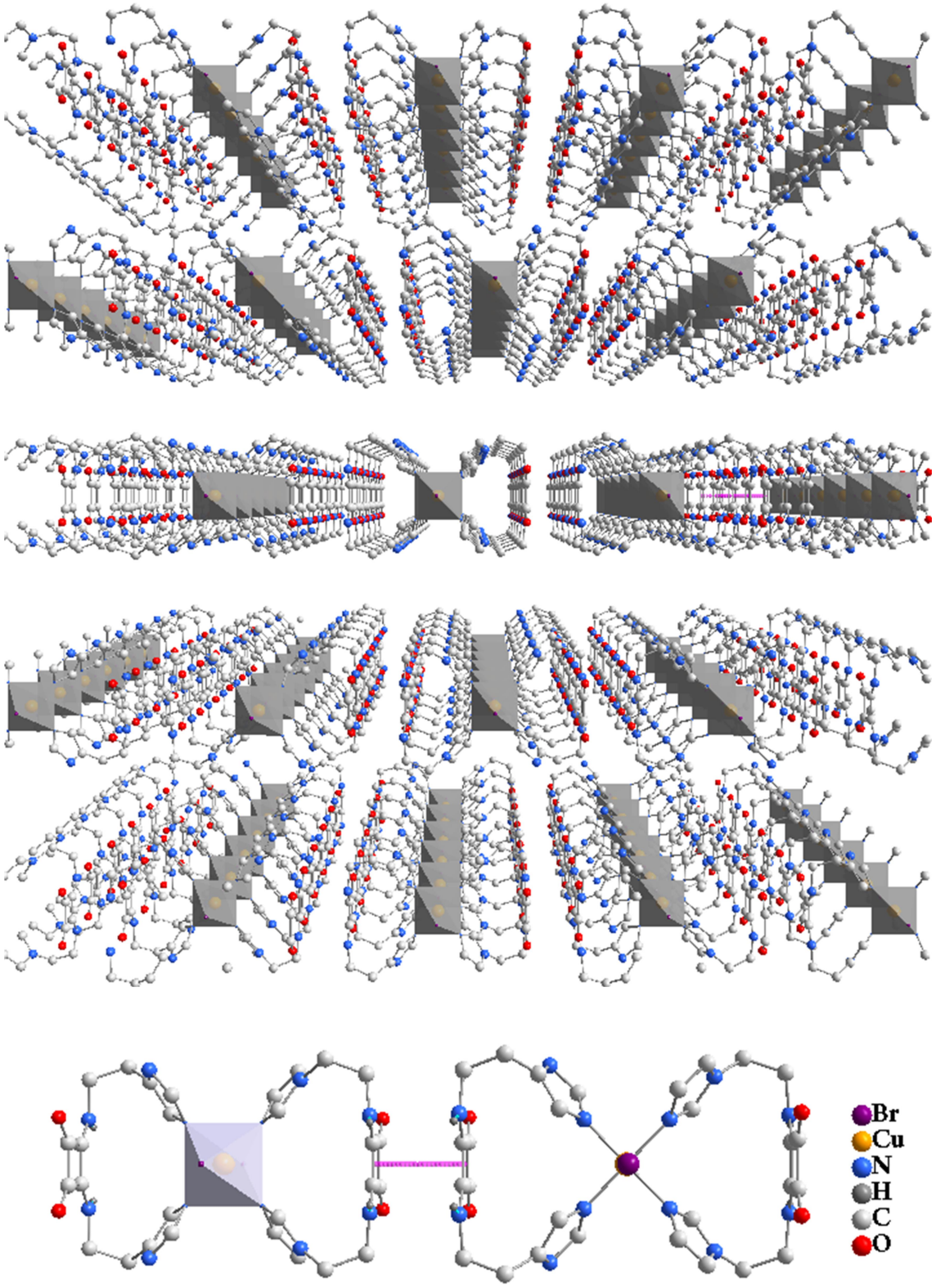

Figure S6 The packing structure of [Cu-**L4**$_2$]Br$_2$ in crystals viewed along *a*-axis (top) with enlarged details (bottom).

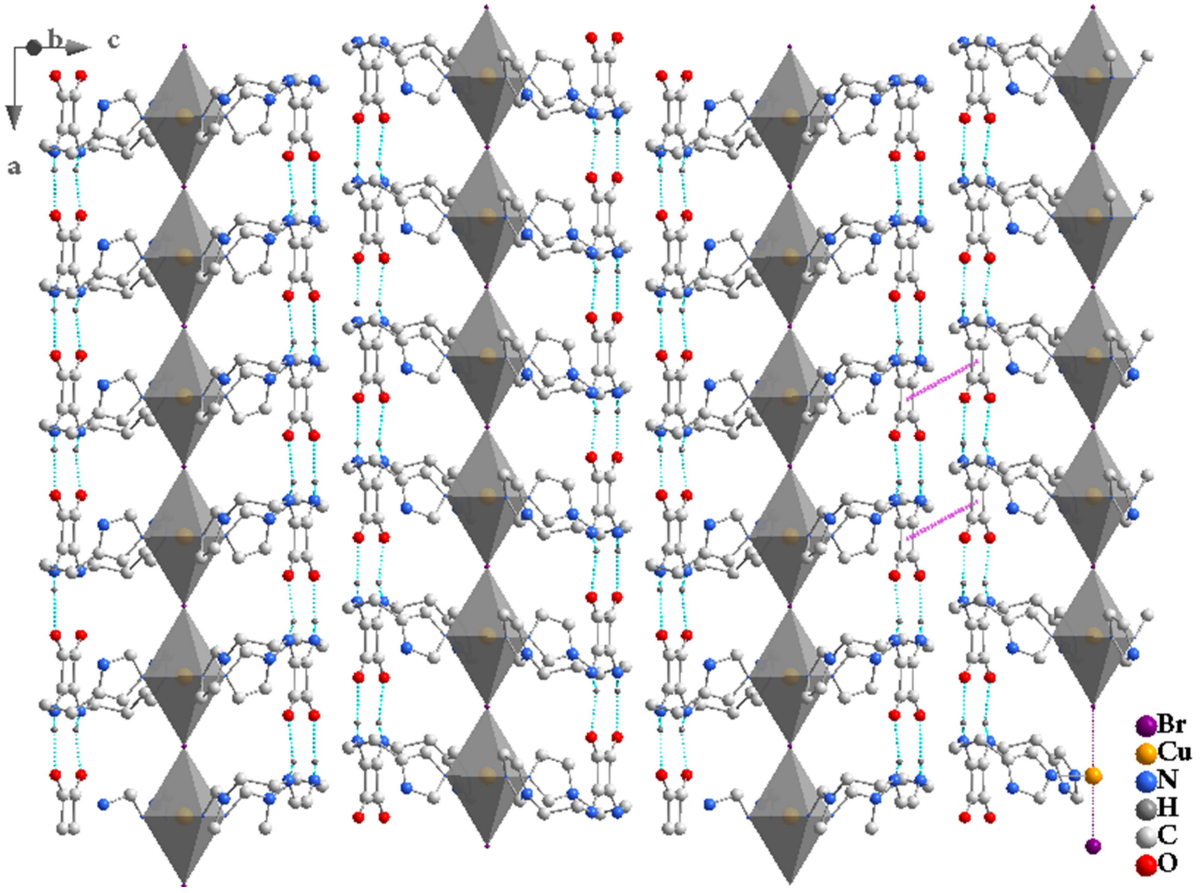

Figure S7 The packing structure of [Cu-**L4**$_2$]Br$_2$ in crystals viewed along *b*-axis, rotated by 20° along *a*-axis.

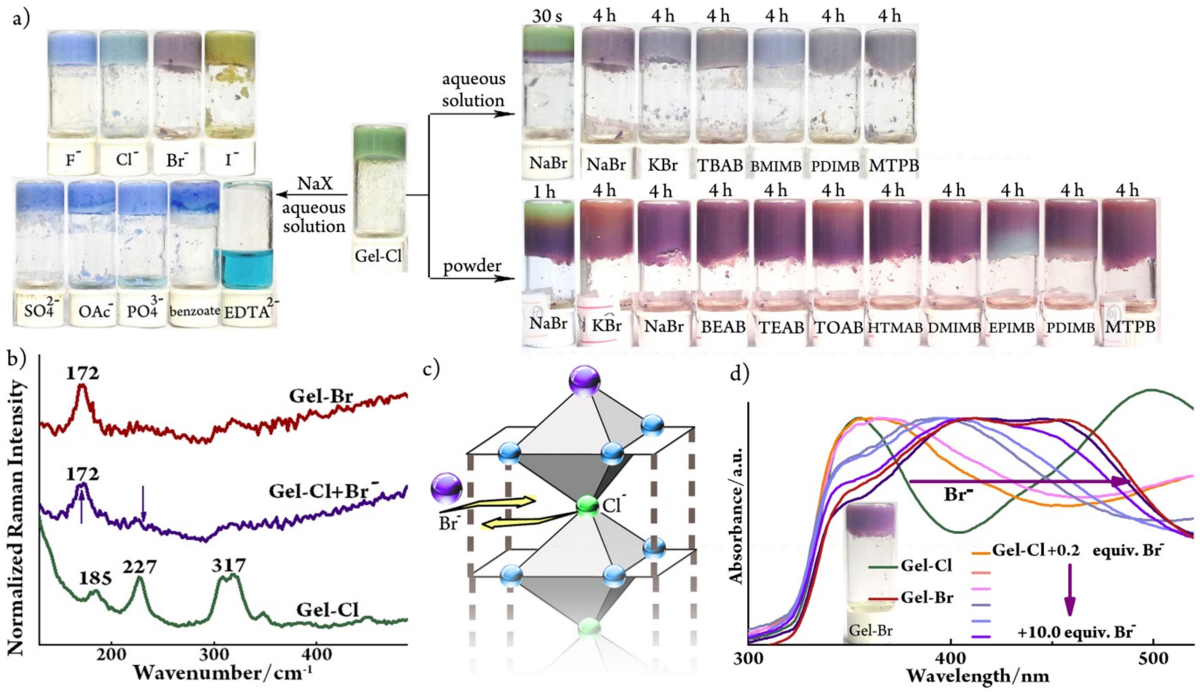

Figure S8. (a) Samples of **Gel-Cl** upon addition of aqueous sodium salts (2.4 mol/L, 70 μL), aqueous bromide salts (2.4 mol/L, 70 μL) and bromide powders (10.0 equiv). For the samples upon the addition of aqueous sodium salts, photos were taken at 4 hours. (b) Raman and (d) DR-UV-*vis* spectra of **Gel-Br** and **Gel-Cl** before and after adding NaBr. **Gel-Cl** and **Gel-Br** gel samples were subject to Raman and DR-UV-*vis* spectrascopy directly. The sample **of Gel-Cl + Br$^-$** was prepared by mixing solid NaBr (10 equiv relative to Cl species in **Gel-Cl**) with **Gel-Cl** and placed overnight for Raman measurement. 0.2, 0.7, 1.3, 2.5, 5.0 and 10.0 equiv of solid NaBr (relative to Cl species in **Gel-Cl**) were mixed, respectively, with **Gel-Cl** and placed overnight for DR-UV-*vis* test. (c) Schematic representation of anion ligand exchange. Blue: N; green: Cl; purple: Br.

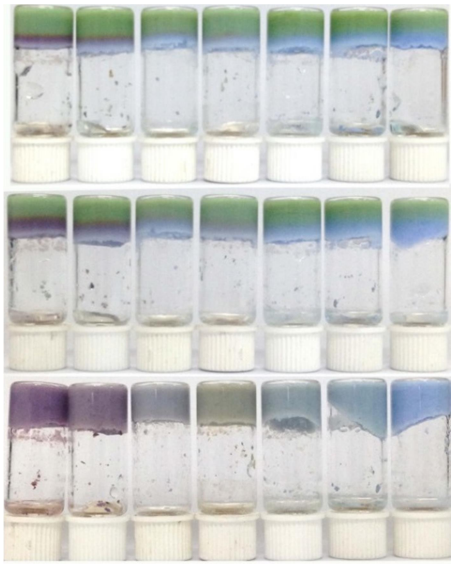

Figure S9 30 seconds (1st row), 2 h (2nd row) and 4 h (3rd row) after **Gel-Cl** was exposed to 10, 5.0, 2.5, 1.3, 0.60, 0.30 and 0.0 equiv (from left to right) of NaBr in H_2O (70 μL, 4.8, 2.4, 1.2, 0.60, 0.30, 0.15 and 0.0 mol/L, respectively).

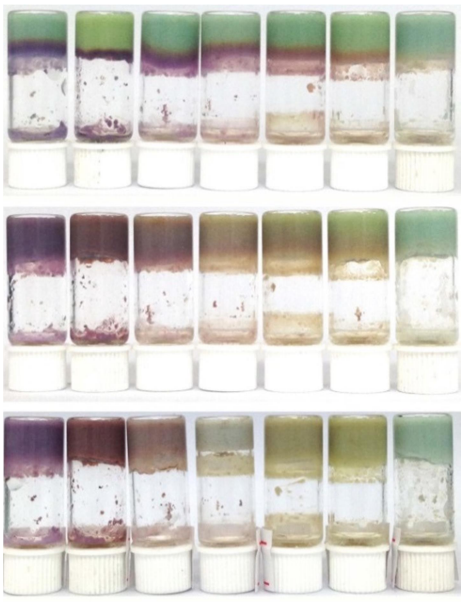

Figure S10 30 seconds (1st row), 4 h (2nd row) and 5 days (3rd row) after **Gel-Cl** was exposed to 5.0, 2.5, 1.3, 0.60, 0.30, 0.15 and 0.075 equiv (from left to right) of NaBr in MeOH (80 μL, 4.2, 2.1, 1.0, 0.50, 0.25, 0.13 and 0.065 mol/L, respectively).

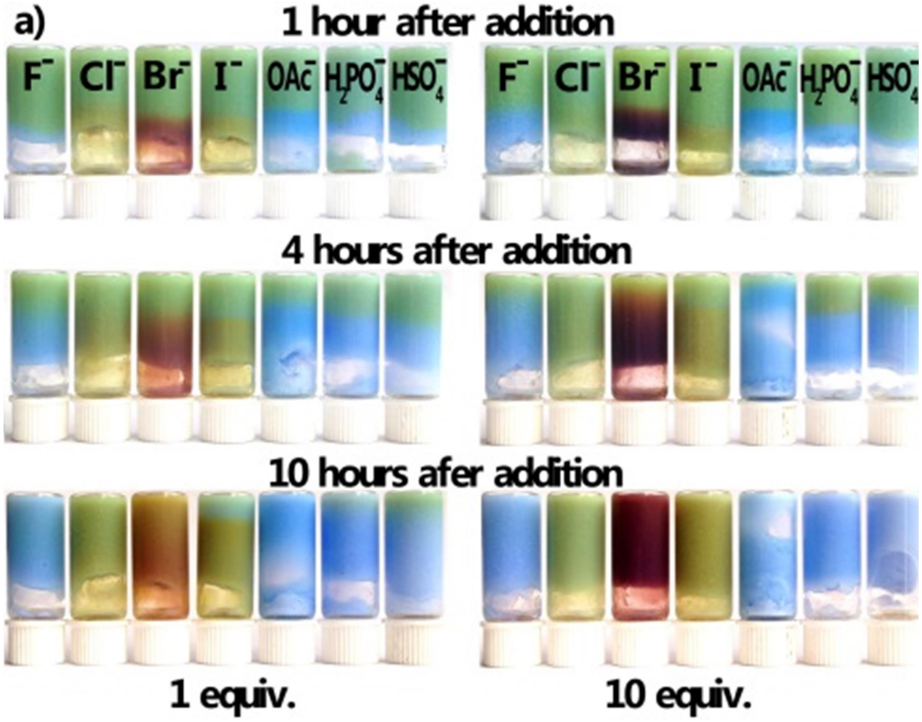

Figure S11 Gel-Cl was exposed to tetrabutylammonium (TBAX) salt powder. Species of X^- and equivalents of X^- were marked in the photos.

Figure S12 Samples of **Gel-Cl** with KBr, NaBr, BEAB, TEAB, TOAB, HTMAB, DMIMB, EPIMB, PDIMB and MTPB solid (10.0 equiv) upon addition of TBAC after 90 days (10.0 equiv, from left to right).

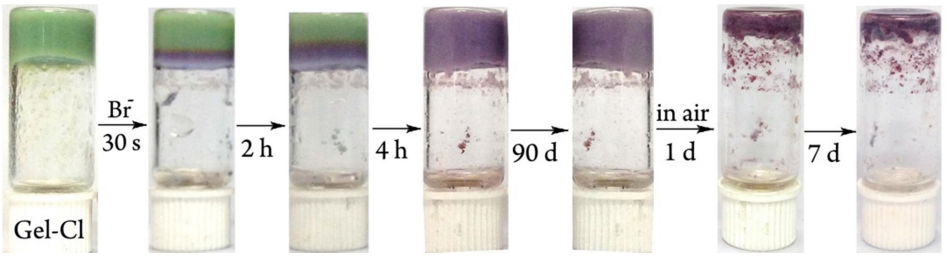

Figure S13 Transformations of **Gel-Cl** upon adding an aqueous NaBr solution (70 μL, 4.8 mol/L).

III. Calculations

The density functional theory (DFT)/B3LYP calculation were performed using Gaussian 09 package.[S1] The crystal structures obtained from the SXRD were used for the single point calculations with a Lanl2DZ basis set on Cu and 6-31G** basis set on the rest of the atoms (C, N, O, H, Cl, Br).

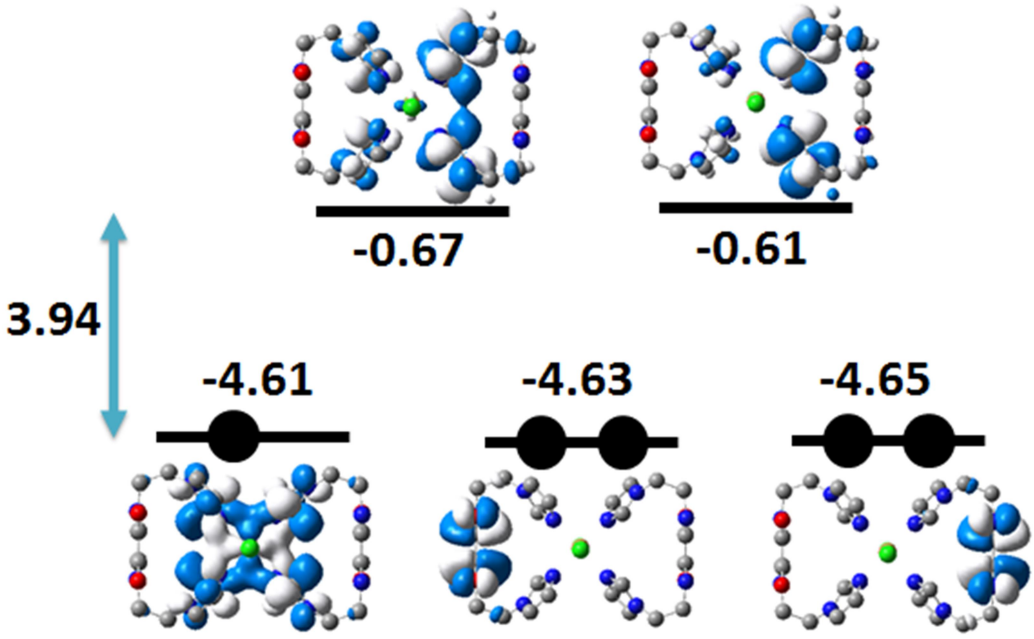

Figure S14 Energy level (eV) and lobes of the front obitals of the complex [Cu-**L4**$_2$]Cl_2.

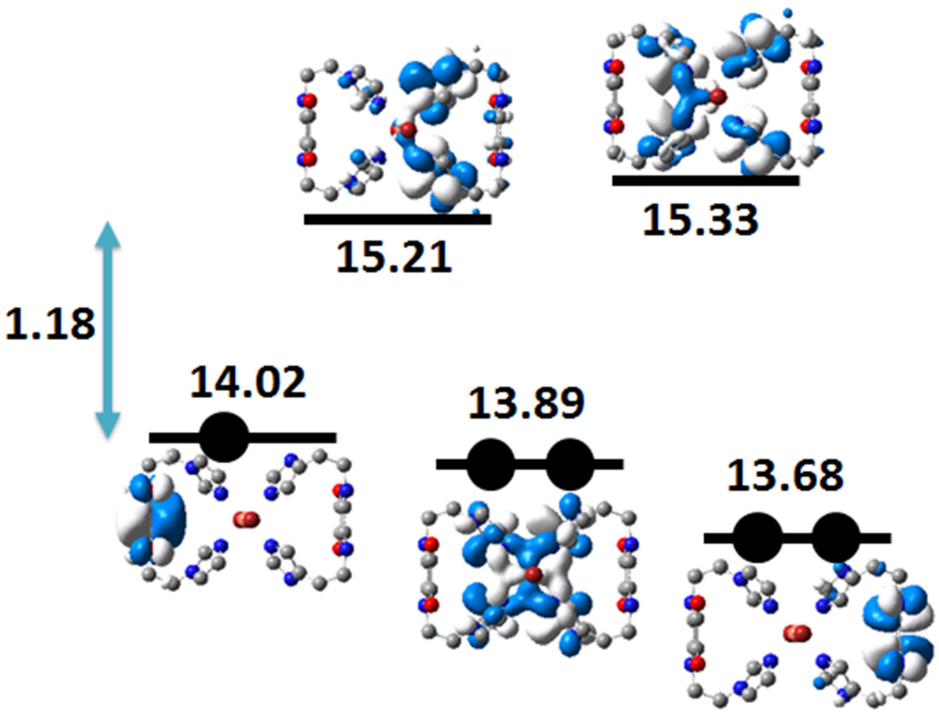

Figure S15 Energy level (eV) and lobes of the front obitals of the complex [Cu-**L4**$_2$]Br$_2$.

References

S1. M. J. Frisch, G. W. Trucks, H. B. Schlegel, G. E. Scuseria, M. A. Robb, J. R. Cheeseman, V. G. Zakrzewski, J. A. Jr. Montgomery, R. E. Stratmann, J. C. Burant, S.Dapprich, J. M. Millam, A. D. Daniels, K. N. Kudin, M. C. Strain, O. Farkas, J. Tomasi, V. Barone, M. Cossi, R. Cammi, B. Mennucci, C. Pomelli, C. Adamo, S. Clifford, J. Ochterski, G. A. Petersson, P. Y. Ayala, Q. Cui, K. Morokuma, D. K. Malick, A. D. Rabuck, K. Raghavachari, J. B. Foresman, J. Cioslowski, J. V. Ortiz, B. B. Stefanov, G. Liu, A. Liashenko, P. Piskorz, I. Komaromi, R. Gomperts, R. L. Martin, D. J. Fox, T. Keith, M. A.Al-Laham, C. Y. Peng, A. Nanayakkara, C. Gonzalez, M. Challacombe, P. M. W. Gill, B. Johnson, W. Chen, M. W. Wong, J. L.Andres, C. Gonzalez, M. Head-Gordon, E. S. Replogle and J. A. Pople, Gaussian 03, Revision D.01, Gaussian, Inc., Pittsburgh PA, **2005**.

III. Copies of ^{1}H and ^{13}C NMR spectra

^{1}H NMR spectrum of 2-(*1H*-imidazol-1-yl)ethanamine in $CDCl_3$

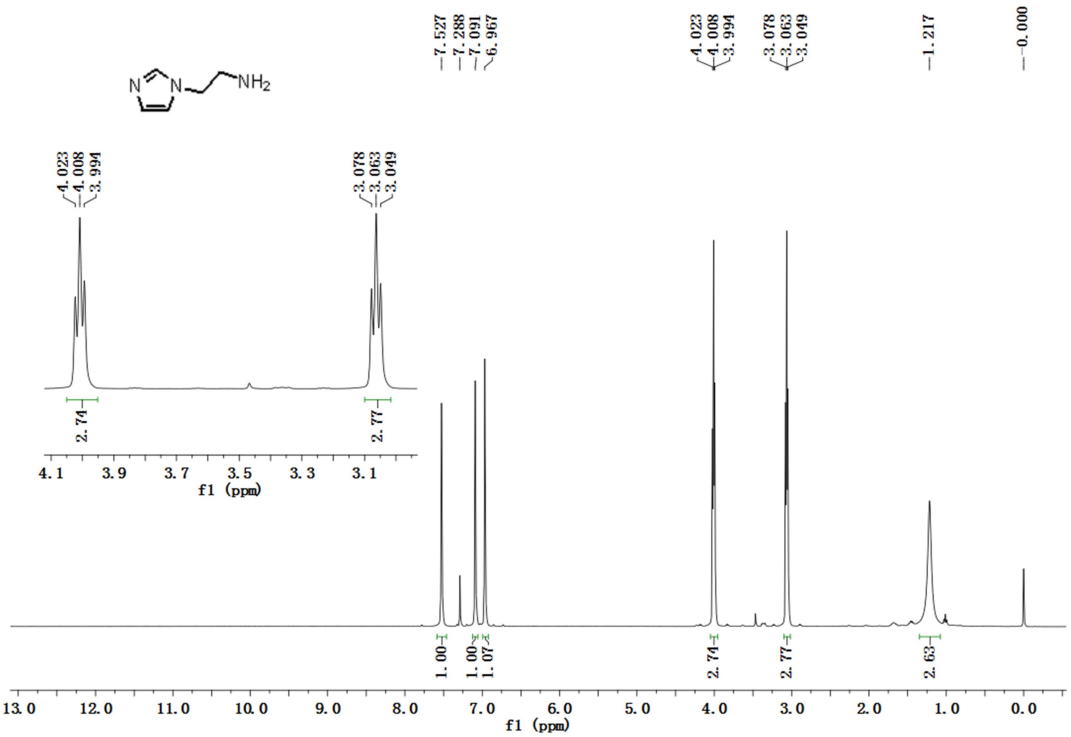

^{13}C NMR spectrum of 2-(*1H*-imidazol-1-yl)ethanamine in $CDCl_3$

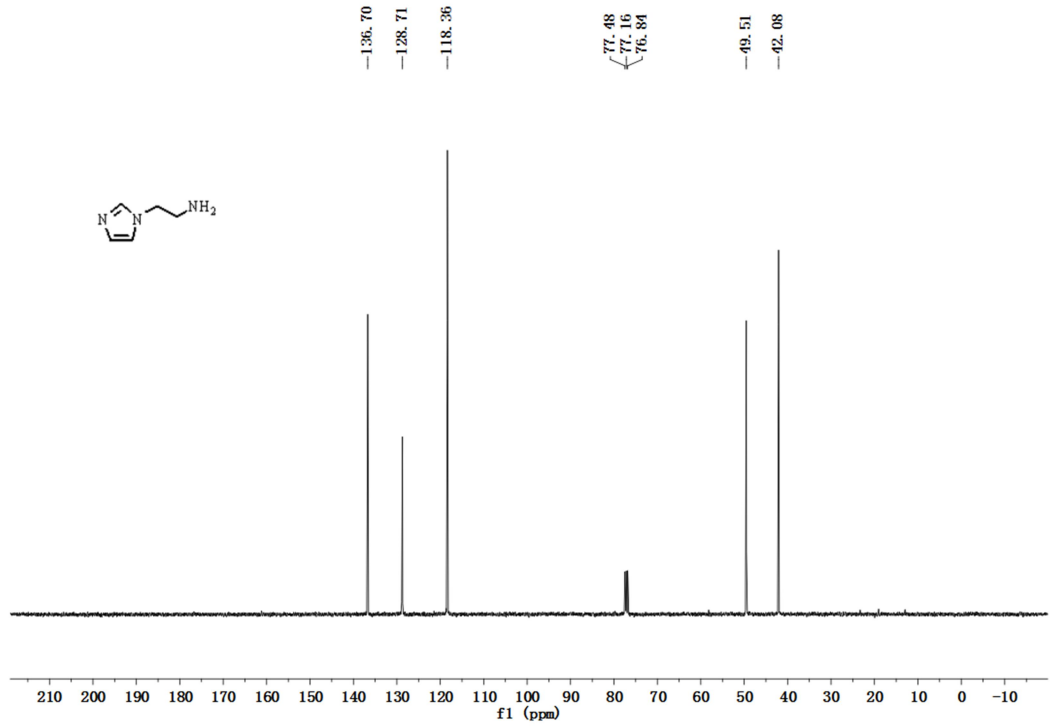

^{1}H NMR spectrum of **L4** in DMSO-d_6

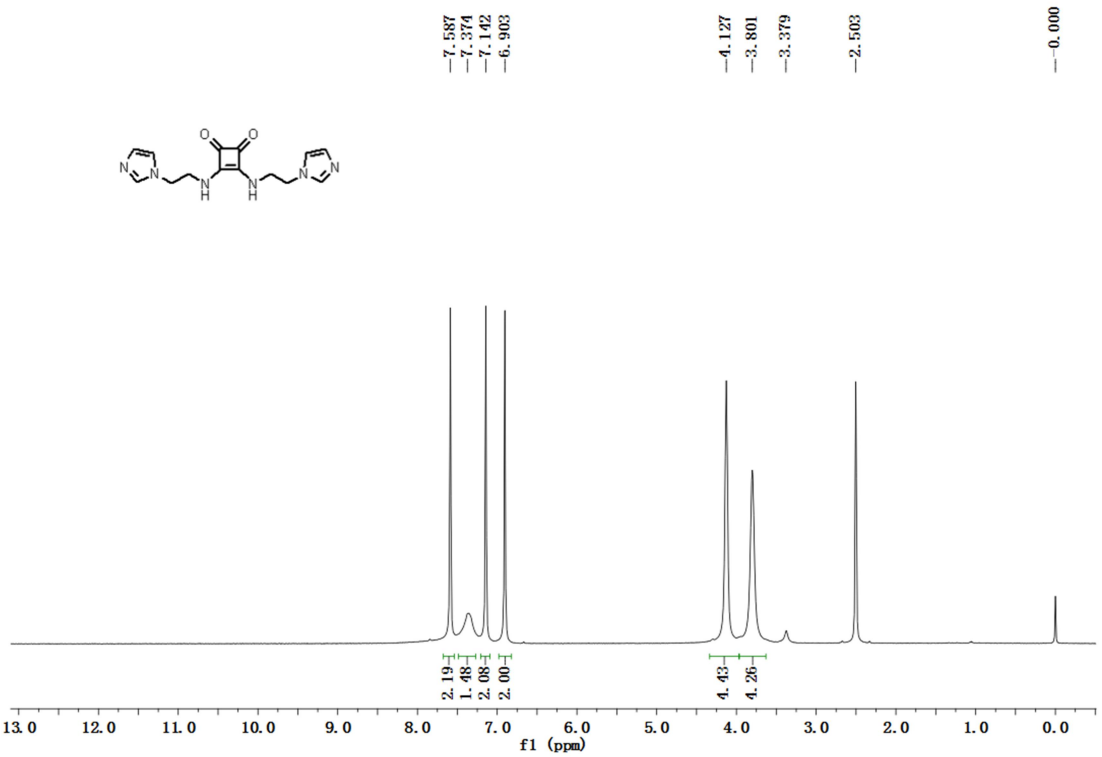

^{13}C NMR spectrum of **L4** in DMSO-d_6

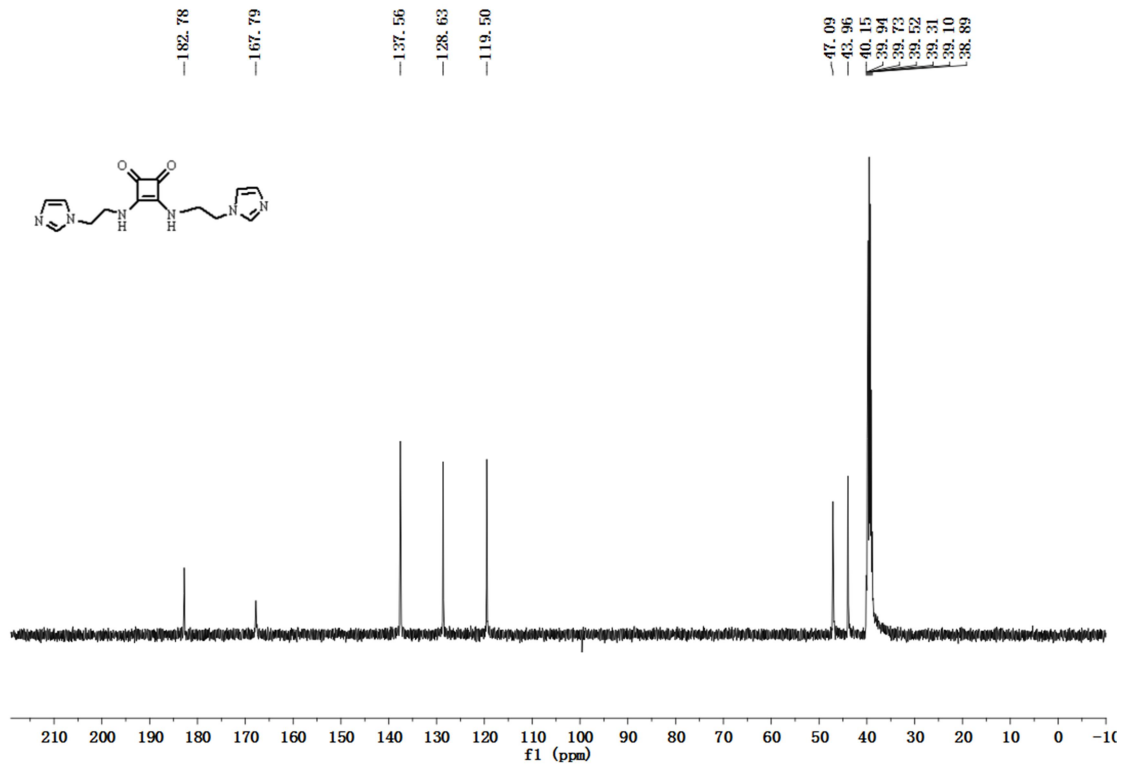

^{1}H NMR spectrum of **L5** in DMSO-d_6

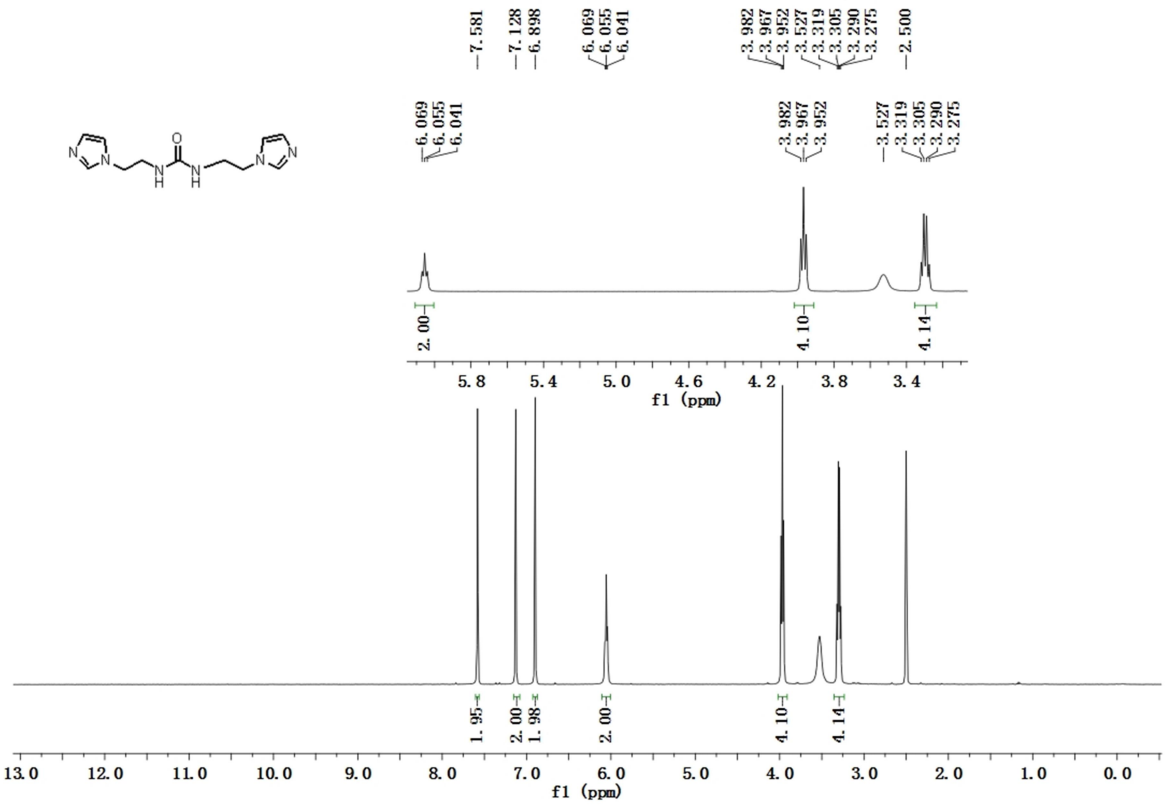

^{13}C NMR spectrum of **L5** in DMSO-d_6